Nanoscale

PAPER

View Article Online
View Journal | View Issue

Cite this: *Nanoscale*, 2014, **6**, 2228

Smart polymer brush nanostructures guide the self-assembly of pore-spanning lipid bilayers with integrated membrane proteins

G. Wilhelmina de Groot,†[a] Sophie Demarche,†[bc] M. Gabriella Santonicola,*[ad] Louis Tiefenauer[b] and G. Julius Vancso*[a]

Received 8th October 2013
Accepted 29th November 2013

DOI: 10.1039/c3nr05356c

www.rsc.org/nanoscale

Nanopores in arrays on silicon chips are functionalized with pH-responsive poly(methacrylic acid) (PMAA) brushes and used as supports for pore-spanning lipid bilayers with integrated membrane proteins. Robust platforms are created by the covalent grafting of polymer brushes using surface-initiated atom transfer radical polymerization (ATRP), resulting in sensor chips that can be successfully reused over several assays. His-tagged proteins are selectively and reversibly bound to the nitrilotriacetic acid (NTA) functionalization of the PMAA brush, and consequently lipid bilayer membranes are formed. The enhanced membrane resistance as determined by electrochemical impedance spectroscopy and free diffusion of dyed lipids observed as fluorescence recovery after photobleaching confirmed the presence of lipid bilayers. Immobilization of the His-tagged membrane proteins on the NTA-modified PMAA brush near the pore edges is characterized by fluorescence microscopy. This system allows us to adjust the protein density in free-standing bilayers, which are stabilized by the polymer brush underneath. The potential application of the integrated platform for ion channel protein assays is demonstrated.

Introduction

Membrane proteins inserted into or attached to lipid bilayer membranes are the gatekeepers of cells and therefore the largest class of drug targets. More than 60% of the pharmaceutical compounds currently on the market target membrane proteins.[1,2] Among these targets, ion channels that mediate passive ion translocation across cell membranes are especially relevant, as they are involved in many essential biological processes, including signal transmission for controlling muscle or cardiac cell contraction.[3] Biosensor surfaces having pore-spanning lipid bilayers with integrated membrane proteins are expected to significantly improve the high-throughput screening of drug candidates.[4–6] Due to their ion transport function, the class of transmembrane ion channels would particularly benefit from integration into porous platforms, as access to both sides of the proteins can simplify their screening, as well as the scientific investigation of the diverse structure–function relationships of these proteins.[7]

There are many challenges in the development of biosensors for membrane protein screening. The surface property is one important factor and appropriate chemical modification of supports enhances fusion of liposomes resulting in supported bilayers.[7] Artificial lipid membranes obtained by liposome fusion are preferred over lipid membranes from painting lipids dissolved in organic solvents, as residual aliphatic molecules might interact with the membrane proteins and impair their function. Moreover, membrane protein systems reconstituted over solid nonporous surfaces have several disadvantages. First, a solid support might impede the protein functionality by a direct contact, and secondly the accumulation of ions in the space between the bilayer and the support leads to fast saturation and causes low sensitivity for analytical electrochemical applications.[3] Silicon-based membranes with predetermined pore arrays have been used to achieve stable and functional painted lipid bilayers.[8] In that work, the long-term stability of lipid bilayers was investigated for several lipids, and the bilayer functionality confirmed by electrochemical measurement after insertion of the potassium transporter valinomycin.

Schmitt and colleagues reported the chemical modification of a nanoporous platform to promote liposome fusion into a free-standing, solvent-free lipid bilayer with a membrane resistance too low to record the single channel activity but high enough for the collective activity of ion channel ensembles.[9] A cholesterol derivative was chemisorbed *via* a thiol end group to

[a]*Materials Science and Technology of Polymers, MESA+ Institute for Nanotechnology, University of Twente, 7500 AE Enschede, The Netherlands. E-mail: g.j.vancso@utwente.nl*

[b]*Laboratory of Biomolecular Research, Paul Scherrer Institute, 5232 Villigen PSI, Switzerland*

[c]*Laboratory of Biosensors and Bioelectronics, Institute of Biomedical Engineering, ETH Zürich, 8092 Zürich, Switzerland*

[d]*Department of Chemical Engineering Materials and Environment, Sapienza University of Rome, 00184 Rome, Italy. E-mail: mariagabriella.santonicola@uniroma1.it*

† These authors contributed equally to this work.

the porous alumina substrates and large unilamellar vesicles (LUVs) were fused on the surface. Recently, Korman *et al.* described nanopore-spanning lipid bilayers over a Si_3N_4 pore array of 40 000 pores.[10] Prior to the lipid bilayer formation from rupture of small unilamellar vesicles (SUVs) of 200 nm diameter, the silicon nitride membrane with pores of 130 nm was functionalized by an organosilane layer to achieve a hydrophobic surface. The membrane fluidity of the established lipid bilayer was assessed by fluorescence recovery after photobleaching (FRAP) and found to be comparable to similar bilayers deposited on silanized glass. A high electrical resistance (>1 GΩ) was measured by electrochemical impedance spectroscopy (EIS). However, it is questionable if such hydrophobic nanoporous surfaces are useful as supports for lipid bilayers with embedded transmembrane proteins, since the hydrophobic transmembrane domain of the proteins preferentially interacts with the hydrophobic surface.

Polymers, either physically adsorbed or covalently attached to the surfaces, are generally used as cushions for supporting lipid membranes on solid supports.[11,12] In the work by Sugihara and colleagues a lipid bilayer is formed over a pore of 800 nm diameter filled with a polyelectrolyte multilayer (PEM).[13] The filling prevents diffusion of the small unilamellar vesicles (50 nm diameter) through the pore, and the lipid bilayer is preferentially formed at the top side of the chip. Fusion to PEMs is promoted if oppositely charged lipids are used for the liposomes. Such polymer-supported bilayers exhibit an increased lifetime and a high membrane resistance. Moreover, the PEM is permeable for monovalent ions. The use of charged polymers to induce the rupture of lipid vesicles made of zwitterionic lipids (net charge zero) on functionalized surfaces has recently been investigated by our group. A zwitterionic polymer layer of sulfobetaine methacrylate (SBMA) was covalently grafted from initiator molecules bound to the surface using atom transfer radical polymerization, and a supported lipid bilayer was formed from fusion of DOPC liposomes.[14] The DOPC membranes on poly(SBMA) layers showed high fluidity and stability as determined by fluorescence microscopy and AFM investigations.

A major bottleneck in the development of membrane protein assays is to integrate proteins into a free-standing bilayer over pores, so that both sides of the bilayer are accessible to the aqueous compartments and proteins are not impeded by interaction with the supporting surface. Specific coupling chemistries offer an efficient way to control the location of proteins on surfaces, most notably *via* the selective and reversible immobilization of His-tagged proteins to NTA-modified interfaces. This approach is used to create protein patterns on the micrometer and nanometer scale,[15] and to immobilize membrane proteins within a supported lipid bilayer allowing structural investigations,[16–18] or functional studies of the proteins.[19–21] Polymers are often chosen as interfaces for modification with NTA groups and subsequent protein immobilization.[22,23] To our knowledge, however, a pore-spanning lipid membrane with integrated membrane proteins over the pores is yet to be demonstrated.

In this study we present a novel system featuring a controlled immobilization of membrane proteins in free-standing lipid bilayers suspended on nanopores. We first functionalize the inner walls of the nanopore array of a silicon nitride membrane with pH-responsive poly(methacrylic acid) (PMAA) brushes and further modify these with nitrilotriacetate groups. The nanopore functionalization with pH-sensitive polymer brushes allows the opening and closing of pores on command. Chemical modification was achieved by surface-initiated atom transfer radical polymerization (SI-ATRP), a versatile controlled polymerization technique that allows for the synthesis of robust polymer architectures on surfaces.[24–26] Recently, we have demonstrated the functionalization of nanopore arrays with PMAA brushes using SI-ATRP, and we used the pH-driven reversible switching of the polymer brush as a way to control ion permeability across the nanopores.[27] This work and other previous studies from our group[28] showed that under physiological conditions negatively charged PMAA brushes swell and fill the pores. Another advantage of the functionalization with PMAA brushes is the availability of the carboxylic acid groups that can be coupled to the amine group of the NTA moiety after activation by *N*-(3-dimethylaminopropyl)-*N*′-ethylcarbodiimide hydrochloride/*N*-hydroxysuccinimide (EDC/NHS).[29] We use this modification to position liposomes with integrated His-tagged membrane proteins, specifically bacterial ion channels NaChBac (from *Bacillus halodurans*) and KvAP (from *Aeropyrum pernix*), above the pores. This study presents the next logical step towards controlled transport through membrane protein assays, which would finally enable a selective pharmaceutical screening using membrane proteins.

Results and discussion

Functionalization of nanopore chips with NTA–PMAA brushes

The nanopore array chips have a silicon nitride surface that was first functionalized with PMAA brushes using surface-initiated ATRP of sodium methacrylate, and subsequently the carboxylic acid groups of the polymer were activated and coupled to aminobutyl NTA *via* EDC/NHS chemistry (Scheme 1). The PMAA brush functionalization was performed on the *trans* side of the nanopore chips (Fig. 1a).

During vapor phase deposition of the ATRP initiator, the *cis* side of the chips was placed on a protecting PDMS layer. In the subsequent processes, the polymer brush is synthesized only on the *trans* side of the chip surface, as well as on the walls of the nanopores. This procedure was used to functionalize only the area around the nanopores on one side of the chips.

Nanopore chips with a pore size of 200 nm were chosen to match the extent of the swollen PMAA brush in the physiological buffers used for the proteolipid membranes, therefore providing a polymer support for the membrane assembly on the porous platform. This estimate was based on previous work from our group on the pH-induced pore switching between closed and open states after PMAA brushes were grafted from the nanopore walls under similar conditions.[27] At the same time, nonporous silicon substrates were functionalized in parallel to the nanopore array chips to check the grafting of the polymer brushes by various surface-sensitive techniques. Typically, surface-initiated ATRP was conducted for one hour, resulting in PMAA brushes of a thickness of 177 ± 5 nm, as

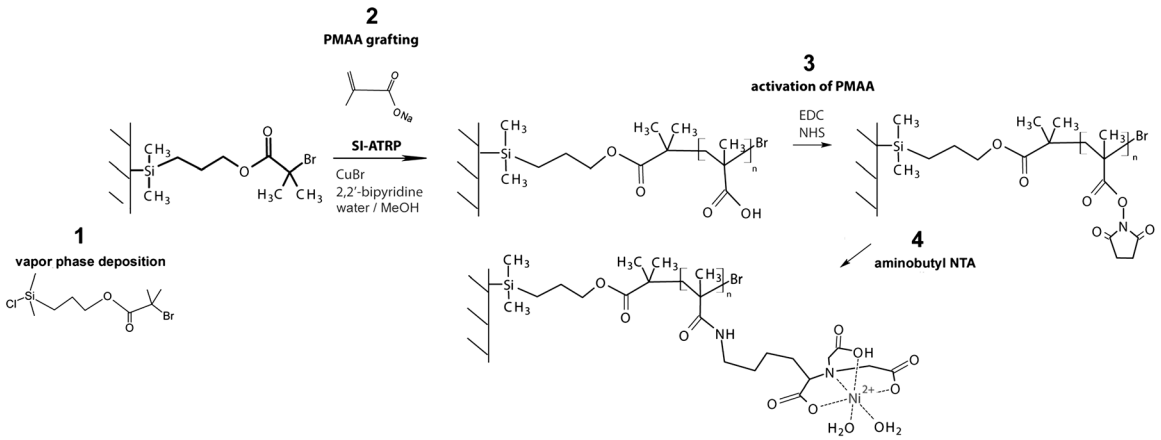

Scheme 1 Reaction scheme of the functionalization of silicon nanopore chips with NTA-modified PMAA brushes: (1) immobilization of the ATRP initiator (3-(2-bromoisobutyryl)propyl)dimethylchlorosilane on the pre-activated silicon surface by vapor phase deposition; (2) synthesis of PMAA brushes by surface-initiated ATRP of sodium methacrylate; (3) conversion of the carboxylic acid groups of PMAA into an active ester by *N*-(3-dimethylaminopropyl)-*N*′-ethylcarbodiimide hydrochloride (EDC) and *N*-hydroxysuccinimide (NHS); (4) reaction of the ester with aminobutyl NTA.

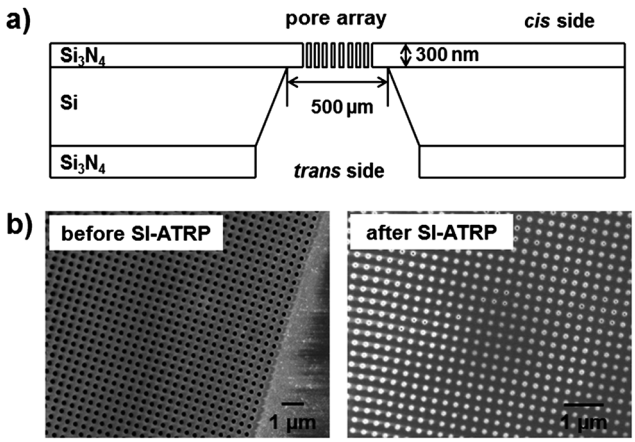

Fig. 1 (a) Cross-sectional scheme of the nanopore array chips used in this study. The nanopores are generated in a 300 nm thick silicon nitride membrane with an area of 0.5 × 0.5 mm^2. (b) SEM images of an array chip at the *cis* side (pore diameter 200 nm) before and after surface-initiated grafting of the PMAA brush.

measured by ellipsometry in air. SEM images were taken at the *cis* side of the nanopore chips before and after polymerization from the *trans* side (Fig. 1b). No conductive coating was deposited on the chips to avoid modification of the grafted polymer layer. The SEM images of the nanopores after surface-initiated ATRP confirm that the PMAA brush (the white non-conductive part in Fig. 1b) is grafted from the nanopore walls all the way through to the *cis* side of chips.

His-tagged proteins were added to the covalently attached NTA moiety present within the pores in the presence of Ni^{2+} ions. Derivatization of the carboxylic acid groups of PMAA by aminobutyl NTA was confirmed by Fourier transform infrared (FTIR) spectroscopy. Fig. 2 shows the FTIR spectra of PMAA brushes before and after NTA coupling in the carbonyl absorption region. Both spectra were obtained after immersing the sample for 15 minutes in a phosphate solution of pH 8 to ensure that most of the carboxylic acid groups were deprotonated (absorbance band at 1558 cm^{-1}). Under this condition the absorbance signal from the characteristic peptide C=O stretch at 1685 cm^{-1} (the amide I band) is prominent avoiding contribution from the unreacted protonated carboxylic acid groups (absorbance band at approximately 1705 cm^{-1}). The spectra confirm the presence of the amide group and thus a successful coupling of NTA to the PMAA brush. Measurements of water contact angles in advancing mode on the nonporous silicon surface functionalized with a PMAA brush before and after NTA coupling gave values of 5.4 ± 2° and 6.5 ± 3°. This indicates that the hydrophilicity of the brush-coated surfaces has not changed by the NTA aminobutyl coupling.

The immobilization of a His-tagged protein to the NTA-modified PMAA brush was investigated by fluorescence confocal microscopy (Fig. 3). A nonporous flat substrate was functionalized with the PMAA brush and subsequently modified with the NTA moiety, only on one half of the surface. Next,

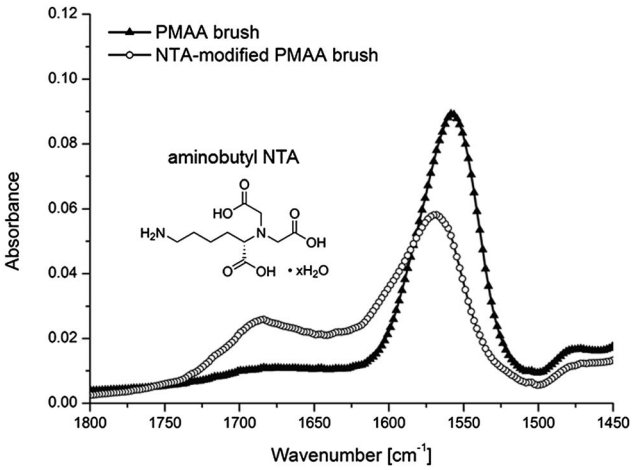

Fig. 2 Transmission FTIR absorbance spectra of a PMAA-brush functionalized nonporous silicon surface in the carbonyl region, before and after coupling with aminobutyl NTA *via* EDC/NHS activation.

the chip was first incubated with a solution containing Ni^{2+} ions and then with His-tagged green fluorescent protein (His-GFP) as a model protein.

Fig. 3a clearly shows the fluorescence of His-GFP immobilized exclusively on the area where NTA moieties are present. In addition, the immobilization of the purple His-mCherry-NaChBac to the NTA-modified PMAA brush is shown (Fig. 3b). By rinsing the sample with a solution of EDTA, the protein is released from the surface and the fluorescence intensity decreased by 92% (Fig. 3c and d). These results confirm the specific and reversible immobilization of the His-proteins to the NTA moiety, which allows for the efficient regeneration of the NTA-modified polymer surface.

Fluorescence confocal microscopy of nanopore-spanning lipid membranes

Nanopore array chips with 16 384 pores, each of 200 nm diameter, were functionalized with NTA-modified PMAA brushes as described (see the Experimental section). The *cis* side of the polymer functionalized chips was incubated overnight in a suspension of POEPC/NBD-PC (97%/3%) liposomes of 50 nm diameter. After incubation, the chips were rinsed with buffer solution and imaged by fluorescence confocal microscopy.

Fig. 4 presents fluorescence confocal measurements after incubation of the liposomes with NTA–PMAA-functionalized nanopore arrays and a control with a polymer-free chip for comparison. The fluorescence images confirm the presence of the lipids on the *cis* side of the nanopore chip. In the control (Fig. 4b), only very low fluorescence is detectable indicating that the liposomes are almost completely detached by the washing step. In Fig. 4a, the slightly uneven distribution of the fluorescent intensity across the chip surface may be an indication that the lipid membrane is not completely flat over the polymer-functionalized nanopores. The surface-initiated polymerization that we used for the synthesis of the PMAA brush is well controlled, generating polymer structures that are homogenous in length to the order of ±5 nm, as confirmed by ellipsometry measurements. However, given the small thickness of the lipid bilayer (3–4 nm),[30] even such a low polydispersity in polymer brush growth may not be sufficient for a flat pore-spanning lipid membrane.

During fluorescence experiments, lipid membrane formation over the PMAA brush was investigated using positively charged POEPC liposomes of different sizes ranging from 50 nm to 400 nm. The best results in terms of fluorescence intensity detected from the pore-spanning membrane were obtained when POEPC liposomes of 50 nm diameter fused to the negatively charged PMAA brush at physiological pH. It should be noted that the lipid membrane only forms on the *cis* side of the 200 nm-wide nanopores, even when liposomes of 50 nm diameter are used. In fact, at physiological pH the nanopores are completely filled with the swollen PMAA brush and are not permeable to the liposomes. Previously, we had reported an investigation of the protonation of pH-responsive PMAA brushes grafted from silicon surfaces, both neat and porous, as a function of pH.[17] The pK_a value of the carboxylic acid groups of the PMAA brush was 6.5, meaning that the polymer brush is negatively charged, and thus swollen when immersed in buffers under physiological conditions (pH 7.4). The effect of pH variations on the configuration of PMAA brushes grafted from nanopores was also analyzed in AFM experiments. The investigations demonstrated that the 200 nm-wide pores were closed at pH higher than 6.5 and open at lower pH values.[27]

In order to confirm that liposomes have really fused and are not just attached to the surface we investigated the pore-

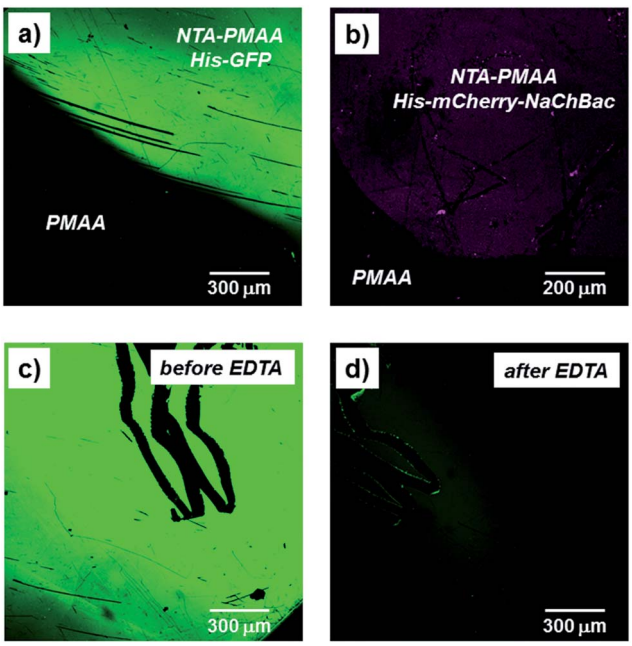

Fig. 3 Top: fluorescence confocal images of the PMAA brush grafted from a nonporous silicon surface partially functionalized with NTA after incubation with (a) His-GFP (green) and (b) His-mCherry-NaChBac (purple). Bottom: silicon surface functionalized with a NTA–PMAA brush after incubation with His-GFP (c), and after subsequent incubation in EDTA solution (0.5 M) for 10 min (d). The black pattern in (c) and (d) is a scratch used as a reference area.

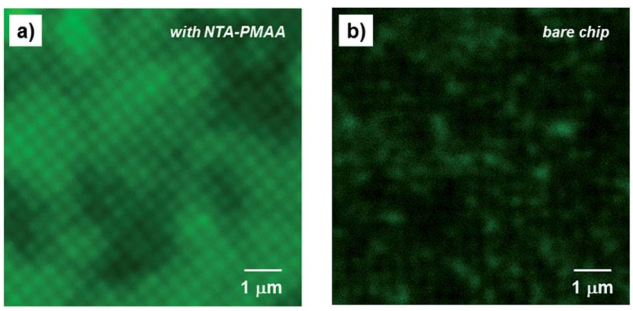

Fig. 4 Fluorescence confocal images of a positively charged POEPC/NBD-PC (97%/3%) membrane on a nanopore array chip with a pore diameter of 200 nm (a) functionalized with the NTA-modified PMAA brush and (b) without the polymer brush. The brighter fluorescent areas of (a) are the pore-spanning part of the lipid membrane. Nanopore chips are imaged from the *cis* side, on which lipid membrane formation occurs after liposome incubation at room temperature overnight.

spanning membranes using fluorescence recovery after photobleaching (FRAP). A circular area with a diameter of ~10 μm was bleached by laser and the recovery of dyed lipids, which is related to the lipid mobility within the membrane, was followed over time. Fig. 5 shows an example of a FRAP measurement of a bilayer lipid membrane spanned over a NTA–PMAA-functionalized nanopore array chip. From the FRAP recovery curves, the diffusion coefficient (D) of the labeled NBD-PC lipid was determined following the procedure by Axelrod *et al.*[31] Three replicate samples were taken, and for each sample an average D value was calculated from a minimum of four bleached spots in different regions of the nanopore array. The D values were found to be $0.38 \pm 0.14\ \mu m^2\ s^{-1}$, $0.32 \pm 0.14\ \mu m^2\ s^{-1}$, and $0.12 \pm 0.04\ \mu m^2\ s^{-1}$, respectively, for the three samples. The recovery of lipids within the bleached area was relatively fast and completed in less than four minutes, thus confirming the presence of a continuous lipid bilayer membrane formed on the NTA–PMAA brush modified nanopores. For comparison, these D values are higher than the ones obtained for lipid bilayer membranes over nanopore chips filled with polyelectrolyte multilayers ($D = 0.08 \pm 0.04\ \mu m^2\ s^{-1}$),[13] and they are closer to the values reported for free lipid membranes as those of liposomes in solution ($D = \sim 1\ \mu m^2\ s^{-1}$).[32] As can be expected, the values of the lipid diffusion coefficients in polymer-supported bilayers will be lower than those in liposomes since the negatively charged PMAA brush interacts electrostatically with the positively charged lipids.

The rate of lipid diffusion within the membrane is an important measure to assess its quality and potential usefulness for biosensor applications, as the membrane fluidity may be a crucial factor to retain the activity of the reconstituted proteins. However, lipid diffusion coefficients determined on nanopore arrays should be judged with caution, as they include contributions from the free-standing part of the membrane as well as from the part that is in contact with the solid edges of the nanopores.[33]

Electrochemical impedance spectroscopy of single-nanopore spanned lipid membranes

In addition to FRAP measurements, electrochemical impedance spectroscopy was used to confirm lipid bilayer formation. Measurements of single-nanopore spanned lipid membranes by EIS gave information on the membrane sealing properties and electrical resistance. Silicon chips with a single pore of 200 nm diameter were functionalized with NTA–PMAA brushes, charged with Ni^{2+} ions, and then incubated with the POEPC liposomes at room temperature overnight. EIS spectra were acquired after extensive rinsing. Before incubation in the liposome suspension, the bare nanopore chips and the NTA–PMAA brush functionalized chips were measured. In most cases, the total resistance increased. Since both the pH and ionic strength of the system remained constant, it can be assumed that the resistance change is due to the lipid bilayer membrane formation on the nanopore. EIS measurements were repeated up to four hours after the end of the liposome incubation, and no further significant change was observed. Fig. 6 shows a representative set of EIS spectra before and after the formation of the nanopore-spanning lipid membrane. The bare single-pore chip has a slightly lower impedance than the chip functionalized with the NTA-modified PMAA brush. This is likely related to the presence of negative charges on the PMAA brush at the physiological pH values of the buffer. At the lowest frequency, the impedance is dominated by the lipid membrane resistance. Several PMAA-brush functionalized chips were incubated overnight in the POEPC liposome

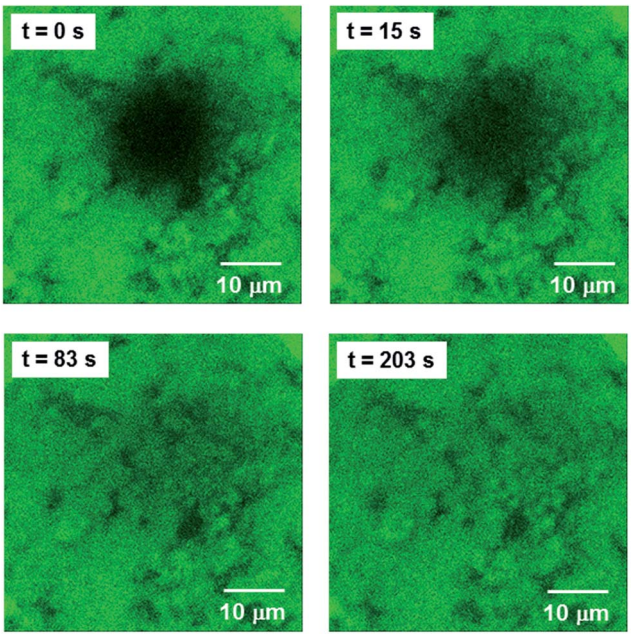

Fig. 5 Fluorescence recovery after photobleaching (FRAP) experiment of a positively charged POEPC/NBD-PC (97%/3%) bilayer membrane spanned over an array of nanopores functionalized with NTA-modified PMAA brushes.

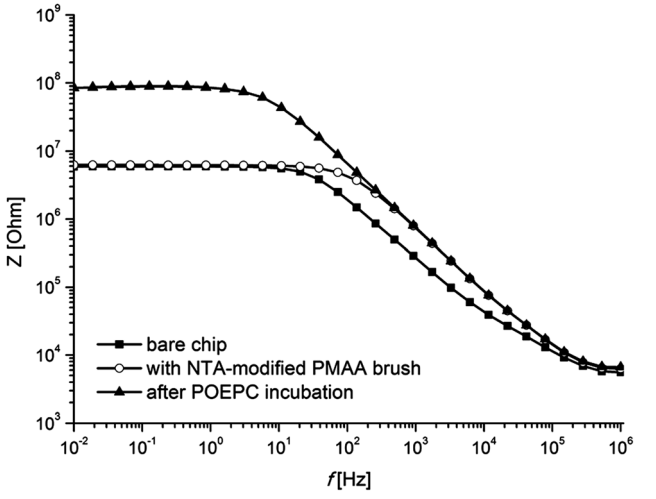

Fig. 6 Electrochemical impedance spectra before and after formation of a POEPC lipid membrane on a chip with a single pore of 200 nm diameter. The solution of POEPC liposomes was incubated over the nanopore chip at room temperature overnight.

solutions. The rate of the bilayer lipid membrane formation with a resistance higher than 50 MΩ was 76%.

To investigate the role of the liposome charge on the lipid membrane formation over the PMAA-functionalized nanopores, EIS measurements were also performed using mixed liposomes containing different ratios of POEPC (positively charged) and POPC (zwitterionic) lipids. Analysis of the impedance spectra indicated that formation of the pore-spanning lipid membrane, at physiological pH values, occurred only when liposomes with at least 80% of POEPC were used. This critical POEPC content that is necessary for the mixed liposomes to fuse on the PMAA-functionalized nanopores is strictly dependent on the pH of the buffer solution, since that determines the net charge on the pH-responsive polymer. Pore-spanning POPC/POEPC membranes with different compositions can then be made to fuse on the porous chips by varying the solution pH.

Nanopore-spanning lipid bilayers with integrated His-tagged membrane proteins

The integration of membrane proteins into preformed lipid bilayers and with both sides of the protein accessible to aqueous compartments is still difficult to achieve, and is thus a limiting factor in the development of biosensors of membrane proteins. In our concept a proteolipid membrane is formed on top of an NTA-functionalized nanoporous support, which allows for the immobilization of His-tagged membrane proteins near the pore edges. In this study we used His-tagged bacterial ion channels, His-NaChBac and His-KvAP, whose functional purification was previously demonstrated by our group.[34,35] Bacterial ion channels represent good models in the screening and functional studies of this class of proteins, due to their abundance and simpler purification procedure than the human homologues. In particular, NaChBac and KvAP are voltage-gated ion channels that open to sodium and potassium ions, respectively, upon depolarization of the lipid bilayer. Two different protocols for the formation of the proteolipid membrane were investigated.

(1) His-NaChBac protein was immobilized on the NTA-modified PMAA brush of the nanopore array chip and the lipid membrane was formed after liposome incubation. For fluorescence confocal microscopy, His-mCherry-NaChBac was delivered to the nanopore chips in the buffer used for protein purification. This buffer contains a detergent (DDM, 0.03% w/v), commonly used to solubilize membrane proteins in aqueous solutions to maintain the 3D structure and functionality.[36–38] After one hour of incubation, the solution on the *cis* side of the nanopores was replaced by a solution of POEPC liposomes containing fluorescent TopFluor-PC (3% mol) and left overnight. Following extensive rinsing, the nanopore chips were inspected by fluorescence confocal microscopy to detect the fluorescent signals from both components, the protein and the lipid of the proteolipid membrane. Excitation at 488 nm and emission at 503–523 nm showed the TopFluor-labeled lipids, whereas excitation at 543 nm and emission at 550–650 nm allowed the detection of the mCherry-labeled protein. Images by fluorescence microscopy in Fig. 7 clearly show that both the His-tagged membrane proteins and the lipid membrane are integrated into the nanopore array chip. Further, FRAP measurements allow us to compare the fluidity of the lipid membrane containing the His-NaChBac protein to that of the protein-free POEPC membrane. The lipid diffusion coefficient D for the proteolipid membrane decreased from 0.27 ± 0.14 $\mu m^2\ s^{-1}$ to 0.22 ± 0.07 $\mu m^2\ s^{-1}$ when the protein was incubated at a concentration of 25 $\mu g\ mL^{-1}$, and to 0.06 ± 0.03 $\mu m^2\ s^{-1}$ when the protein was incubated at 250 $\mu g\ mL^{-1}$. As expected, the presence of proteins in the lipid membrane lowers its fluidity. This can be ascribed to the hydrophobic and electrostatic interactions between the embedded membrane proteins and the surrounding lipids, which decreases the lipid mobility. This effect is more pronounced, as more protein is included in the pore-spanning lipid membrane. However, the obtained D values are still consistent with the presence of a lipid bilayer.[39]

Pore-spanning lipid membranes were formed on single-pore chips with immobilized His-NaChBac proteins and analyzed by electrochemical impedance spectroscopy. EIS spectra revealed an increase in electrical resistance of the chips after membrane formation up to 97 MΩ, confirming the formation of the lipid membrane adjacent to the immobilized membrane proteins.

(2) To further simplify the process and to reduce the risk of membrane protein denaturation during immobilization onto the nanopore chip, we formed the suspended proteolipid membrane by direct rupture of preformed proteoliposomes of POEPC containing the His-tagged membrane protein KvAP (1/200 w/w) in the lipid bilayer. The successful integration of the protein into the proteoliposomes was previously assessed by recording the ion channel activity in the black lipid membrane. After incubation of the proteoliposomes over the nanopore chips modified with the Ni-NTA–PMAA brush, the EIS spectra showed a lipid bilayer resistance over 90 MΩ in at least 50% of the experiments, thus confirming a proteolipid membrane formation over the polymer-functionalized pore arrays directly from fusion of proteoliposomes. A third attempt was not successful: His-tagged membrane proteins embedded in mixed micelles of lipids and detergent and the subsequent removal of the detergent molecules by Bio-beads™ led to membranes with resistance below 30 MΩ.

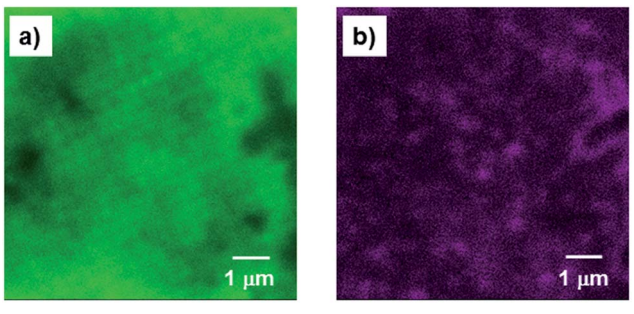

Fig. 7 (a) Fluorescent confocal image of the lipid component of a proteolipid membrane with POEPC/TopFluor-PC (97%/3% by mol) and His-mCherry-NaChBac suspended over nanopores functionalized with the NTA–PMAA brush. (b) Fluorescence from the His-mCherry-NaChBac protein integrated into the nanopore-spanning membrane.

The function of ion channels reconstituted in artificial lipid bilayers can be measured by electrochemical methods when a high membrane sealing is achieved on the support, so that the background noise, that is the current due to ions moving through the membrane defects, is sufficiently low as compared to the current passing through the ion channel. Previously, the activities of NaChBac and KvAP were measured in artificial lipid bilayers prepared on bare porous surfaces by the painting method.[34,35] Such artificial membranes were characterized by very high resistance values (~1 GΩ). These values cannot be matched in our current work due to the presence of the swollen polymer layer in contact with the proteolipid membrane. However, to verify if the lipids used in our study could adversely affect the functionality of the proteins, we formed black lipid membranes fusing proteoliposomes containing POEPC and His-KvAP as described above to a POEPC/POPC membrane. By forming this black lipid system, the KvAP activity could be measured and confirmed.

One of the significant advantages of our concept is that the sensor surface can be regenerated. Nanopore chips modified with the NTA–PMAA brush after bilayer formation were regenerated by cleaning with ethanol; chips with membrane proteins were cleaned with EDTA solution (0.5 M) and protein cleaning solution containing pepsin. EIS measurements of reused nanopore chips showed that a pore-spanning lipid membrane with an electrical resistance of 100 MΩ was obtained even after seven regenerations of the same chip also when incubated with proteins.

Conclusions

Silicon nanopore chips were functionalized with NTA-modified PMAA brushes to generate a useful platform for free-standing lipid membranes with integrated membrane proteins. On the nanopore array, the immobilization of the His-tagged membrane proteins was controlled using the NTA moiety present on the polymer brush. In a physiological buffer, the pH-responsive PMAA brush ($pK_a = 6.5$) was swollen and filled the pores, thus favoring the formation of free-standing POEPC membranes. The lipid membrane was fluid and with an electrical resistance up to 142 MΩ, as demonstrated in FRAP and EIS experiments.

An optimal procedure for the formation of the proteolipid membrane was found by immobilization of the His-tagged protein on the NTA-modified polymer brush followed by direct rupture of the POEPC liposomes. For pore-spanning lipid membranes containing His-NaChBac, it was also demonstrated in FRAP experiments that the protein density could be varied in a wide range (25–250 μg mL^{-1}) without impairing the formation of the lipid bilayer. This approach offers several advantages over previously reported pore-spanning lipid membranes: (1) it enhances the probability of suspending organic solvent-free POEPC lipid bilayers from liposome fusion on the nanoporous surface and (2) enables the controlled location of membrane proteins integrated into lipid membranes; (3) the covalent grafting of the PMAA brush *via* surface-initiated polymerization resulted in a universal platform for His-tagged membrane protein assays and (4) allowed the repeated use of the nanopore chips; (5) this design could be particularly useful for measuring the activity of ion channels, under conditions where the PMAA brush is in its neutral (collapsed) state and the nanopores are permeable to ions.

The electrical resistance achieved using the integrated sensor platform of this investigation was in the best case one order of magnitude lower than the one of painted bilayers, which poses experimental limitations for the electrochemical activity measurements of the reconstituted ion channels. Nevertheless, our current platform will allow for optical activity measurements of membrane proteins, for which the resistance is not a critical parameter. In the future, several factors, including pore shape and diameter, and the use of lipid mixtures, will be investigated to increase the electrical resistance of the membrane protein assay and enable electrochemical activity measurements.

Experimental

Materials

Allyl 2-bromo-2-methylpropionate (98%), chlorodimethyl-hydrosilane, chloroplatinic acid hexahydrate (≥37.50% Pt basis), CuBr (99.999%), 2,2′-bipyridine (≥99.0%), *N*-(3-dimethylaminopropyl)-*N*′-ethylcarbodiimide hydrochloride (EDC, ≥98.0%), *N*-hydroxysuccinimide (NHS, 98%) and Nα,Nα-bis(carboxymethyl)-L-lysine hydrate (aminobutyl NTA, ≥97.0%) were purchased from Sigma-Aldrich and used without further purification. Sodium methacrylate (99%) was purchased from Sigma-Aldrich and washed with toluene and dried under vacuum before use. 4-(2-Hydroxyethyl)-piperazine-1-ethane-sulfonic acid (HEPES), potassium chloride (KCl), sodium chloride (NaCl), sodium phosphate monobasic (NaH_2PO_4) and nickel chloride ($NiCl_2$), and protein cleaning solution for electrodes (HI 7073L, HANNA Instruments Inc., USA) were also purchased from Sigma-Aldrich. *N*-Dodecyl-β-D-maltopyranoside (DDM) was purchased from Affymetrix (Santa Clara, USA). His-tagged green fluorescent protein (His-GFP) was purchased from BioVision (San Francisco, USA). 1-Palmitoyl-2-oleoyl-*sn-glycero*-3-ethylphosphocholine (POEPC), 1-palmitoyl-2-(12-[(7-nitro-2-1,3-benzoxadiazol-4-yl)amino]dodecanoyl)-*sn-glycero*-3-phosphocholine (NBD-PC) and 1-palmitoyl-2-(dipyrromethaneboron difluoride) undecanoyl-*sn-glycero*-3-phosphocholine (TopFluor-PC) were purchased from Avanti Polar Lipids (Alabaster, USA). Working buffers with 10 mM HEPES and 150 mM KCl at pH 7.4 were prepared in Milli-Q water (Millipore Corporation, Darmstadt, Germany) and filtered through a 0.2 μm filter. All solvents were of high purity, and deionized water from a Milli-Q purification system (Millipore Advantage A10) was used throughout. Phosphate solutions (50 mM phosphate) with a pH value of 8 were prepared by titrating a stock solution (pH 7.4) using KOH solution.

Nanopore functionalization with NTA–PMAA brushes

Chips with an array of pores or with a single pore accessible on both sides in a 0.5 × 0.5 mm^2 window with a 300 nm-thick silicon nitride membrane were fabricated by Leister Process

Technologies (Axetris).[40] Chips with 16 384 pores (pitch 0.4 μm) of 200 nm diameter and 1 pore of 200 nm diameter were used. Nanopore array chips were functionalized by combining ATRP and the "grafting from" approach following a previously published procedure.[28] Briefly, chips were cleaned and activated in piranha solution (H_2SO_4/H_2O_2 70 : 30 v/v) for 30 min (**warning**: piranha solution reacts strongly with organic compounds and should be handled with extreme caution), rinsed with water and ethanol, and dried in a stream of nitrogen. Next, a monolayer of the ATRP initiator (3-(2-bromoisobutyryl)propyl)dimethylchlorosilane was deposited on the pore walls by vapor phase deposition *via* the *trans* side of the chips, while protecting the *cis* side by placing it on a polydimethylsiloxane (PDMS) layer. The SI-ATRP of sodium methacrylate was performed at room temperature for 1 h under an argon atmosphere. Polymerization was performed in a water–methanol mixture 50 : 50 v/v to improve the wetting of the pore walls and to allow for the polymer brush growth inside the nanopores. Sodium methacrylate (50 mmol) was dissolved in the ATRP medium (10 mL) and the solution degassed before addition to a Schlenk flask with CuBr (1 mmol) and 2,2′-bipyridine (2.2 mmol) under an inert atmosphere. After stirring for 15 min, the ATRP mixture was transferred to the argon-filled vials with the initiator-coated nanopore chips. After polymerization, the chips were washed with water and with EDTA solution (0.1 M, pH 7), and then immersed in water overnight to remove any physisorbed polymer. Finally, chips were rinsed with ethanol and dried under nitrogen gas.

The activation of the carboxylic acid groups of the PMAA brushes was performed *via* EDC/NHS chemistry.[41,42] PMAA-brush functionalized nanopore chips were immersed for 30 minutes in a 0.1 M EDC/NHS solution (1 : 1 ratio) in Milli-Q water, rinsed subsequently with Milli-Q water and ethanol, and dried in nitrogen flow. Next, the chips with activated PMAA brushes were immersed for 1 h in a solution of aminobutyl NTA (0.1 M), adjusted to pH 10 with NaOH solution, rinsed with Milli-Q water and dried in nitrogen flow.

Characterization of PMAA brushes

Water contact angle measurements were performed with the sessile drop method, in the static or advancing mode, using the OCA15 instrument (Dataphysics, Germany) equipped with an electronic syringe unit. Milli-Q water was used as the probe liquid and for each sample three successive measurements were made. The polymer brush thickness was measured using a variable-angle spectroscopic ellipsometer (VASE) (J.A. Woollam Co., Lincoln, NE, USA) in the range from 1.5 to 4.5 eV with a step size of 0.1 eV. The measurements were performed at three different incident angles (65°, 70° and 75°), and were averaged over an area of 2 mm^2. The ellipsometry spectra, *i.e.* Ψ and Δ as a function of the wavelength, were analyzed using the software package CompleteEASE (Woollam), employing the tabulated dielectric functions for both silicon and silicon oxide as the substrate. SEM images were taken with a JEOL JSM-6330F field emission instrument operated at 5 kV. No coating with conductive materials was applied on the polymer-functionalized nanopore chips. FTIR spectra were obtained with a Bio-Rad FTS-575C spectrometer equipped with a nitrogen-cooled cryogenic mercury telluride detector (spectral resolution of 4 cm^{-1}, 1024 scans). The background spectrum was obtained by recording the spectrum of a cleaned silicon substrate. The PMAA brush grafted from silicon was investigated by immersing the sample in a phosphate solution of pH 8 for 15 minutes, rinsing it with ethanol, drying it under a nitrogen stream, and placing it in the FTIR spectrometer. The same procedure was repeated after coupling of NTA to the carboxylic acid groups of the PMAA brush.

Protein expression and purification

His-NaChBac and His-mCherry-NaChBac were expressed and purified using a published protocol,[34] with the following modifications. His-NaChBac was genetically modified to carry a mCherry fluorescent protein at its C-terminus, yielding a His-mCherry-NaChBac protein. Gel filtration was performed using a Superdex 200 column (GE Healthcare, Freiburg, Germany). His-NaChBac and His-mCherry-NaChBac were stored at −80 °C in gel filtration buffer (50 mM NaH_2PO_4, 300 mM NaCl, 10% glycerol and 0.03% DDM at pH 8). His-KvAP (from *Aeropyrum pernix*) was expressed and purified as previously described.[35]

Preparation of (proteo)liposomes and incubation

Lipids in chloroform were mixed to the desired ratio in a test tube and chloroform was evaporated under a nitrogen stream (>3 h). Lipids were then hydrated with working buffer (>1 h) to a final lipid concentration of 10 mg mL^{-1} and vortexed. Lipid solutions were extruded 31 times through a polycarbonate filter (Nucleopore Track Etched membranes, GE Healthcare) of the desired liposome diameter: 800 nm, 400 nm, 200 nm or 50 nm. Liposome solutions were stored at 4 °C and used within few days. His-KvAP proteoliposomes (protein/lipid ratio of 1/200 (w/w)) were formed using 100% POEPC liposomes of 50 nm diameter.[35] The functionalized nanopore chips were clamped between two identical poly(methyl methacrylate) (PMMA) compartments of 200 μL with a silicon sealing ring with an aperture exposing the pore array to the compartments. Both compartments were also open at the top side of the module and were filled with working buffer. The *cis* side of the chips was incubated in a $NiCl_2$ solution (20 mM) for 10 min and rinsed 15 times with working buffer. When proteins were incubated during the experiment, the *cis* side of the chips was rinsed with gel filtration buffer, incubated for 1 h with the proteins at the desired concentration, and finally rinsed with gel filtration buffer. Liposome or proteoliposome solutions were diluted to a final concentration of 1 mg mL^{-1} and incubated in the *cis* compartment overnight. Before EIS measurements the compartment was rinsed extensively with working buffer.

Characterization of pore-spanning (proteo)lipid membranes

EIS spectra were acquired using an Autolab PGSTAT 12 (Ecochemie, Utrecht, The Netherlands) equipped with a FRA module. Two Ag/AgCl electrodes were placed in each PMMA

compartment (WPI reference electrode, Lot-Oriel AG, Germany). EIS spectra were recorded from 1 MHz to 0.01 Hz at 0 V offset potential by applying a signal amplitude of 10 mV. EIS measurements were performed in a Faraday cage. Confocal fluorescence microscopy and FRAP investigations were performed with a Leica microscope TCS SP5 (Leica Microsystems, Wetzlar, Germany) equipped with an Ar laser (488 nm), a He–Ne laser (543 nm), and a 63× glycerol objective (Leica Microsystems). Liposomes were prepared with POEPC and NBD-PC or TopFluor-PC as fluorophores (97%/3% by mol). After liposome incubation, the chips were rinsed 30 times with working buffer and placed in a Ludin chamber (Life Imaging Services, Basel, Switzerland) mounted with a sample coverslip of thickness #1 (Menzel-Gläser, Germany). Images were analyzed with FRAP wizard from the LAS AF software (Leica Microsystems). From the recovery curves, lipid diffusion coefficients were calculated according to the theory developed by Axelrod *et al.*[31] Fluorescent images were acquired using the same setup.

Acknowledgements

This research was supported by the European Commission through the FP7 program ASMENA (CP-FP 214666-2). We thank Dr Marco Di Berardino and Olivier Dubochet (Axetris, Switzerland) for providing the nanopore array chips, Dr Ingrid Hutter (PSI) for the purification of KvAP protein, Dr Rolf Jaussi (PSI) for the His-mCherry-NaChBac plasmid, and Prof. Janos Vörös (ETH Zürich) for fruitful discussions. M.G.S. acknowledges financial support from the Italian Ministry of Education, University and Research through the Montalcini Program.

Notes and references

1 J. P. Overington, B. Al-Lazikani and A. L. Hopkins, *Nat. Rev. Drug Discovery*, 2006, **5**, 993.
2 M. Rask-Andersen, M. S. Almén and H. B. Schiöth, *Nat. Rev. Drug Discovery*, 2011, **10**, 579.
3 S. Demarche, K. Sugihara, T. Zambelli, L. Tiefenauer and J. Vörös, *Analyst*, 2011, **136**, 1077.
4 E. Reimhult and K. Kumar, *Trends Biotechnol.*, 2008, **26**, 82.
5 M. Bally, K. Bailey, K. Sugihara, D. Grieshaber, J. Vörös and B. Städler, *Small*, 2010, **6**, 2481.
6 M. Zagnoni, *Lab Chip*, 2012, **12**, 1026.
7 L. Tiefenauer and S. Demarche, *Materials*, 2012, **5**, 2205.
8 X. J. Han, A. Studer, H. Sehr, I. Geissbuhler, M. Di Berardino, F. K. Winkler and L. X. Tiefenauer, *Adv. Mater.*, 2007, **19**, 4466.
9 E. K. Schmitt, M. Nurnabi, R. J. Bushby and C. Steinem, *Soft Matter*, 2008, **4**, 250.
10 C. E. Korman, M. Megens, C. M. Ajo-Franklin and D. A. Horsley, *Langmuir*, 2013, **29**, 4421.
11 M. Tanaka and E. Sackmann, *Nature*, 2005, **437**, 656.
12 M. Tanaka, M. Tutus, S. Kaufmann, F. F. Rossetti, E. Schneck and I. M. Weiss, *J. Struct. Biol.*, 2009, **168**, 137.
13 K. Sugihara, J. Vörös and T. Zambelli, *ACS Nano*, 2010, **4**, 5047.
14 M. G. Santonicola, M. Memesa, A. Meszyńska, Y. J. Ma and G. J. Vancso, *Soft Matter*, 2012, **8**, 1556.
15 N. P. Reynolds, J. D. Tucker, P. A. Davison, J. A. Timney, C. N. Hunter and G. J. Leggett, *J. Am. Chem. Soc.*, 2009, **131**, 896.
16 S. Gupta, J. A. Dura, J. A. Freites, D. J. Tobias and J. K. Blasie, *Langmuir*, 2012, **28**, 10504.
17 S. Todorovic, A. Verissimo, N. Wisitruangsakul, I. Zebger, P. Hildebrandt, M. M. Pereira, M. Teixeira and D. H. Murgida, *J. Phys. Chem. B*, 2008, **112**, 16952.
18 P. Rigler, W.-P. Ulrich and H. Vogel, *Langmuir*, 2004, **20**, 7901.
19 F. Roder, S. Waichman, D. Paterok, R. Schubert, C. Richter, B. Liedberg and J. Piehler, *Anal. Chem.*, 2011, **83**, 6792.
20 K. Ataka, F. Giess, W. Knoll, R. Naumann, S. Haber-Pohlmeier, B. Richter and J. Heberle, *J. Am. Chem. Soc.*, 2004, **126**, 16199.
21 C. Nowak, M. G. Santonicola, D. Schach, J. P. Zhu, R. B. Gennis, S. Ferguson-Miller, D. Baurecht, D. Walz, W. Knoll and R. L. C. Naumann, *Soft Matter*, 2010, **6**, 5523.
22 G. Zhen, D. Falconnet, E. Kuennemann, J. Vörös, N. D. Spencer, M. Textor and S. Zürcher, *Adv. Funct. Mater.*, 2006, **16**, 243.
23 N. B. Eisele, F. I. Andersson, S. Frey and R. P. Richter, *Biomacromolecules*, 2012, **13**, 2322.
24 R. Barbey, L. Lavanant, D. Paripovic, N. Schuwer, C. Sugnaux, S. Tugulu and H. A. Klok, *Chem. Rev.*, 2009, **109**, 5437.
25 K. Matyjaszewski and J. H. Xia, *Chem. Rev.*, 2001, **101**, 2921.
26 S. Edmondson, V. L. Osborne and W. T. S. Huck, *Chem. Soc. Rev.*, 2004, **33**, 14.
27 G. W. de Groot, M. G. Santonicola, K. Sugihara, T. Zambelli, E. Reimhult, J. Vörös and G. J. Vancso, *ACS Appl. Mater. Interfaces*, 2013, **5**, 1400.
28 M. G. Santonicola, G. W. de Groot, M. Memesa, A. Meszynska and G. J. Vancso, *Langmuir*, 2010, **26**, 17513.
29 C. Wang, Q. Yan, H.-B. Liu, X.-H. Zhou and S.-J. Xiao, *Langmuir*, 2011, **27**, 12058.
30 J. F. Nagle and S. Tristram-Nagle, *Biochim. Biophys. Acta*, 2000, **1469**, 159.
31 D. Axelrod, D. E. Koppel, J. Schlessinger, E. Elson and W. W. Webb, *Biophys. J.*, 1976, **16**, 1055.
32 K. Jacobson, *Cell Motil. Cytoskeleton*, 1983, **3**, 367.
33 D. Weiskopf, E. K. Schmitt, M. H. Kluhr, S. K. Dertinger and C. Steinem, *Langmuir*, 2007, **23**, 9134.
34 A. Studer, S. Demarche, D. Langenegger and L. Tiefenauer, *Biosens. Bioelectron.*, 2011, **26**, 1924.
35 I. Hutter, E. Müller, P. M. Kristiansen, S. Kresak and L. Tiefenauer, *Microfluid. Nanofluid.*, 2013, **14**, 421.
36 G. G. Privé, *Methods*, 2007, **41**, 388.
37 M. G. Santonicola, A. M. Lenhoff and E. W. Kaler, *Biophys. J.*, 2008, **94**, 3647.
38 A. M. Seddon, P. Curnow and P. J. Booth, *Biochim. Biophys. Acta*, 2004, **1666**, 105.
39 Z. I. Lalchev and A. R. Mackie, *Colloids Surf., B*, 1999, **15**, 147.

40 L. J. Heyderman, B. Ketterer, D. Bachle, F. Glaus, B. Haas, H. Schift, K. Vogelsang, J. Gobrecht, L. Tiefenauer, O. Dubochet, P. Surbled and T. Hessler, *Microelectron. Eng.*, 2003, **67-8**, 208.
41 J. H. Dai, Z. Y. Bao, L. Sun, S. U. Hong, G. L. Baker and M. L. Bruening, *Langmuir*, 2006, **22**, 4274.
42 L. Sun, J. H. Dai, G. L. Baker and M. L. Bruening, *Chem. Mater.*, 2006, **18**, 4033.